Journal of Industrial and Engineering Chemistry 94 (2021) 368–375

Contents lists available at ScienceDirect

Journal of Industrial and Engineering Chemistry

journal homepage: www.elsevier.com/locate/jiec

Preparation of fully flexible lithium metal batteries with free-standing β-$Na_{0.33}V_2O_5$ cathodes and LAGP hybrid solid electrolytes

Jong Su Han[a], Gil Chan Hwang[b], Hakgyoon Yu[a], Du-Hyun Lim[a], Jung Sang Cho[c,**], Matthias Kuenzel[d,e,**], Jae-Kwang Kim[a,*], Jou-Hyeon Ahn[f]

[a] Department of Energy Convergence Engineering, Cheongju University, Cheongju, Chungbuk 28503, Republic of Korea
[b] Department of Earth System Sciences, Yonsei University, Seoul 03722, Republic of Korea
[c] Department of Engineering Chemistry, Chungbuk National University, Chungbuk 28644, Republic of Korea
[d] Helmholtz Institute Ulm (HIU), Helmholtzstrasse 11, 89081 Ulm, Germany
[e] Karlsruhe Institute of Technology (KIT), P.O. Box 3640, 76021 Karlsruhe, Germany
[f] Departmentof Chemical Engineering and Research Institute for Green Energy Convergence Technology, Gyeongsang National University, 501 Jinju-daero, Jinju 52828, Republic of Korea

ARTICLE INFO

Article history:
Received 23 August 2020
Received in revised form 6 November 2020
Accepted 16 November 2020
Available online 21 November 2020

Keywords:
Flexible lithium metal battery
NVP
Free-standing electrode
LAGP
Hybrid solid electrolyte

ABSTRACT

Safe and flexible batteries are expected to be the enabler for advancing the technology of wearable electronics to an unforeseen level in near future. However, to date the energy density of such devices is rather limited due to the rather large proportion of dead weight and volume to provide good flexibility. To overcome this hurdle, a disruptive change in the battery manufacturing process is needed. Herein, we not only introduce a simple phase inversion method for the preparation of free-standing and flexible β-$Na_{0.33}V_2O_5$ cathodes without metal current collector, but also demonstrate the possibility to integrate those into fully flexible lithium metal batteries. Additionally, employing a LAGP-based hybrid solid electrolyte enables excellent high temperature stability and thus, enhanced safety characteristics of the device. Such integrated flexible batteries exhibit fast and stable lithium-ion storage capabilities, with a large specific capacity of 228 mA h g^{-1} at 0.1 C and excellent cycling stability translating into an outstanding specific energy of 407.8 Wh kg^{-1} on electrode level.

Introduction

Portable electronics have a bright future with an ever-rising interest in wearable and smart devices that assist in improving life quality and are useful for healthcare. For advanced applications the flexibility of such devices is crucial. Hence, it is essential to develop as well flexible energy storage media with improved electrochemical properties that could power this next generation of portable electronic devices [1–3]. Compared to other energy storage devices, such as hydrogen storage systems and supercapacitors, secondary lithium-ion batteries (LIBs) with good flexibility would be the most viable option to power these devices thanks to their good power density and far superior energy density. However, flexible LIBs have not been commercialized yet and rigid batteries are still employed instead. Although there have been reports on flexible LIBs on lab scale, sustaining the flexibility with at the same time good electrochemical properties remains challenging and often results in reduced capacities in comparison to the rigid ones [4–10]. Especially, the energy density of flexible batteries is rather low due to the inherent limitation of thickness to maintain flexibility. Since cathode materials play a vital role in determining the capacity of LIBs, it is desirable to develop novel efficient cathode materials that could assist in providing both enhanced capacity as well as flexibility to the next generation of flexible LIBs.

To achieve this goal, different strategies have been proposed aiming on tailoring the battery electrodes as thin layers, structuring or pattering the current collector and infiltrating the active materials into porous substrates such as fabrics, paper or plastic [11–14]. However, all these methods have in common to reduce the battery's energy density because the introduction of additional dead weight and non-conductive materials, increasing volume and weight of the cell and might even react with the electrolyte [11]. On the positive electrode side, vanadium pentoxide (V_2O_5) has been employed as active material due to its large abundance, reduced cost and high theoretical capacity

*Corresponding author.
**Corresponding author at: Helmholtz Institute Ulm (HIU), Helmholtzstrasse 11, 89081 Ulm, Germany.

https://doi.org/10.1016/j.jiec.2020.11.011
1226-086X/

[15–17]. However, it is still limited by poor cycleability and specific capacity [18,19]. An interesting approach to encounter these issues is the introduction of sodium metal into the structure of vanadium pentoxide yielding β-$Na_{0.33}V_2O_5$ (NVO) [20,21]. NVO displays a complex three-dimensional framework opening up tunnels within the structure. Those tunnels enable easy lithium-ion insertion and extraction and hence, enhance the specific capacity as well as rate performance of the material [22,23]. NVO is typically prepared by hydrothermal, solid-state, sol-gel or flux methods, which however, generally yields materials with very little or almost negligible flexibility while the processes are costly and complicated [23].

In contrast, we employed a simple decomposition method to synthesize NVO that can be processed by a one-step phase inversion technique in presence of a binder like PVdF to yield free-standing and flexible cathode tapes. A similar method has been used by Logan et al. who prepared flexible cathode tapes based on activated carbon as catalyst and PVdF as binder for application in microbial fuel cells [24]. Herein, we report for the first time a one-step phase inversion method for the preparation of flexible and free-standing NVO cathode tapes without the necessity for any rigid substrate to enable the design of a truly flexible battery using a lithium metal anode. Additionally, the NVO electrode processing can be performed in water as cheap and sustainable solvent owing to the high stability of NVO against water and as well high temperature. As a result, the flexible NVO-based lithium metal battery shows excellent electrochemical performance even at elevated temperature (60 °C) and bended-state employing a hybrid solid electrolyte. Moreover, the use of a non-porous NVO cathode and lithium metal anode is beneficial to improve the energy density of such flexible batteries.

Experimental

Disintegration of α-V_2O_5 in an aqueous solution of hydrogen peroxide was carried out in the presence of sodium salt leading to the formation of NVO as reported earlier by Baddour-Hadjean et al. [25]. First, α-V_2O_5 (1 g) and a stoichiometric amount of Na_2SO_4 were mixed in a beaker with water (10 mL). Thereafter, 30 mL of H_2O_2 (30%) was added into the solution. The α-V_2O_5 is dissolved as diperoxo $[VO(O_2)_2]^-$ species, which is unstable in solution. Progressively, it decomposes to monoperoxo $[VO(O_2)]^+$, which is then further hydroxylated to $[VO(OH)_3(OH_2)_2]$ and $[VO_2(OH)(OH_2)_3]$. After 20 min a red solution is obtained, which was dried in an oven at 70 °C for 12 h. The collected particles were heated at 500 °C for 5 h in air atmosphere.

To prepare free-standing cathode tapes, the active material (NVO), conductive carbon (Super P) and binder (PVdF) were stirred in a mixed solvent containing N-methyl pyrrolidone (NMP) and acetone in a ratio of 6:4 to obtain a homogeneous slurry (NVO: Super-P carbon:PVdF 80:10:10). After through mixing, the slurry was spray coated onto a glass plate followed by immersion of the glass plate in a bath of distilled water for around 15 min, until the cathode tape was released from the glass. The tape was then dried for 12 h at 80 °C to obtain the free-standing and flexible NVO cathode (thickness ~20 μm) as illustrated in Fig. 1.

X-ray diffraction (XRD) data were collected in reflection geometry on a Bruker D8 Advance diffractometer using Cu Kα radiation and a monochromator operated at 40 kV. The crystallographic structural properties were obtained by Rietveld refinement. The chemical composition of the prepared samples was characterized by Fourier transform infrared (FT-IR) spectroscopy on a IFS 66/S spectrometer (Bruker Optik GmbH, Germany). X-ray photoelectron spectroscopy (XPS) was performed on a PHI 5500 spectrometer (Physical Electronics, Inc. (PHI), ULVAC-PHI, USA/Japan) with Al Kα radiation (1485.6 eV) at an anode voltage of 13.8 kV. Morphological characterization and elemental mapping was carried out by scanning electron microscopy (SEM) on a Nova NanoSEM 230 (FEI, Thermo Fisher Scientific, USA), equipped with an energy-dispersive X-ray spectrometer (EDS).

Fig. 1. Phase inversion process for current collector-free flexible NVO cathode.

The NVO cathode (loading: 3.41 mg cm^{-2}) was combined with a lithium metal anode and $Li_{1.5}Al_{0.5}Ge_{1.5}P_3O_{12}$ (LAGP)-based hybrid electrolyte (LAGP:PVdF-HFP:additive = 70:15:15 wt.%; with 1.2 M $LiPF_6$ in EC:DEC as additive) to assemble the flexible lithium metal battery (3 × 4 cm pouch cells prepared in an Ar-filled glove box with H_2O and O_2 levels below 10 ppm). The LAGP conducting ceramic was synthesized by solid-state reaction and the LAGP-based hybrid solid electrolyte was prepared by phase inversion method as reported elsewhere [26,27]. Electrochemical impedance spectroscopy (EIS) was measured on an IM6 potentiostat (ZAHNER-Elektrik GmbH & Co. KG, Germany) at open-circuit voltage in a frequency range from 100 mHz to 2 MHz. The electrochemical performance was assessed using an automatic galvanostatic WBCS3000 battery cycler (WonATech, Korea) between 2.0 and 4.0 V at room temperature and 60 °C. The experiments were performed at different currents ranging from 0.1C (0.08 mA cm^{-2}) to 5C (4.0 mA cm^{-2}). The (dis)charge rate of 1C corresponds to a specific current of 234 mA g^{-1} and all given potential values refer to the Li/Li^+ quasi reference redox couple.

Results and discussion

The refined XRD pattern given in Fig. 2a confirms the successful preparation of phase pure and highly crystalline NVO particles (JCPDS No: 24-1155). As indicated in Fig. 2a the representative peaks can well be assigned to the layered NaV_6O_{15} phase. The crystal structure is indexed to a monoclinic symmetry with space group C2/m [21–23]. The calculated lattice parameters are a = 12.7 Å, b = 3.6 Å and c = 10.7 Å, giving rise to a cell volume of around 489.2 $Å^3$. These results are in good agreement with previously reported NVO powders prepared via different synthesis routes and confirm the viability of our simple approach [25,28]. This unit cell volume is lower than reported in literature [21–23,25]. However, the lower cell volume improves the ion diffusion in the crystal structure during electrochemical reaction. As illustrated in Fig. 2b, this monoclinic crystal structure, typical for β-vanadium bronzes, contains tunnels formed by the association of VO_6 and VO_5 frameworks along the b-axis (y direction). These frameworks consist of zig–zag double strings of distorted VO_6 octahedra that form layers within the (a,b) plane by sharing corners among distorted VO_6 octahedrons, as well as shared edges with VO_5 tetragonal pyramids resulting in the tunnels along the b-axis. In detail, the chains of tetragonal pyramids are connected to the octahedral layers through the oxygen atom O5, which is the common edge of the octahedron around V1 and V2. By that, a (V3) O_5 polyhedron is formed with 5-fold square pyramidal coordination [29]. The lithium ions are located on the inside of these tunnels, at four equivalent interstitial sites per unit cell. Additionally, there remain two more tunnel sites for Li intercalation, located in either of the four eight-coordinated sites or four tetrahedral sites per unit cell.

The morphology of as-prepared NVO particles is presented in Fig. 3. The SEM micrographs reveal a rod-like shape of single NVO particles with relatively smooth surface. The rods have a length of

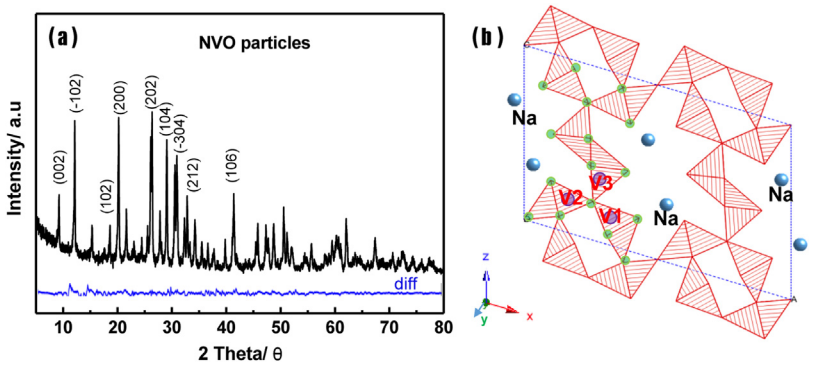

Fig. 2. (a) XRD pattern and (b) crystal structure of NVO particles.

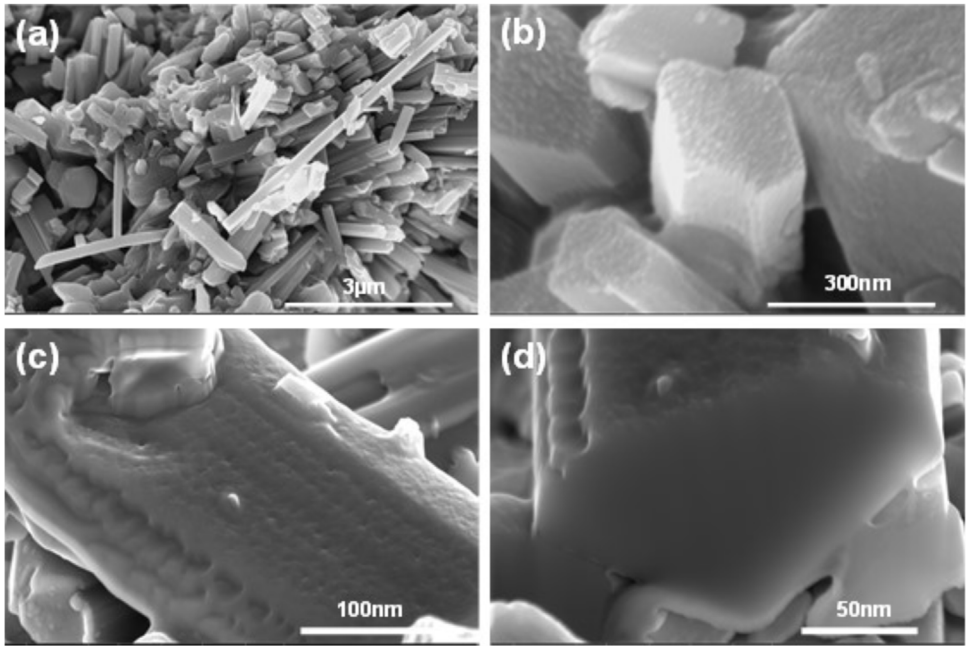

Fig. 3. SEM micrographs of the NVO particles at (a) low (b) intermediate and (c) high magnification as well as (d) in cross-sectional view.

roughly 1–1.5 μm and a width of approximately 0.2–0.3 μm with square shaped area (Fig. 3b). On the surface of the rod-shaped single NVO particles no pores can be found (Fig. 3b, c). The interior of the rods appears to be very dense without any indication for pores as shown by the cross-section in Fig. 3d and supported by TEM micrographs (Fig. S1). Such single particle morphology is beneficial to enhance the tap density as well as energy density in a conventional battery design. Additionally, the particles remain stable in water (see Fig. S2 and corresponding discussion) and the defect free structure allows to expect high electronic conductivity. Therefore, the NVO can easily be processed to prepare flexible electrodes by the phase inversion process using water and could achieve good electrochemical properties without any additional carbon coating process.

Photographs of the obtained flexible and free-standing NVO cathode tape are shown in Fig. 4a. The electrode is highly flexible and does not break easily upon handling. The SEM micrograph in Fig. 4b highlights the strongly cohering electrode network held together by the PVdF binder and the well-distributed conductive carbon particles (see Fig. 4c–g). The uniform distribution of all components is crucial for the electrochemical performance of the electrode. Although PVdF is necessary to hold the electrode together and provide its good flexibility and chemical stability, it is undesirable to cover the whole surface of the electrode to not block ionic transport pathways [24]. At the same time, the presence of conductive carbon helps to guarantee the electron transfer during electrochemical reaction.

To prepare a pouch-type flexible lithium metal battery, the NVO cathode tape is stacked onto a piece of lithium metal foil sticking on a polyimide film and physically separated by a hybrid solid electrolyte (see Figs. S3 and S4 for more information) before soldering and sealing of the pouch cell, as schematized in Fig. 5a. Typically, lithium metal foil is not very flexible and does not return into its initial state once it was bent. However, using a polyimide film as a support, the lithium anode showed high flexibility and could easily revert to its straightened state after bending. The use of lithium anode could provide improved energy density of flexible batteries [30]. To demonstrate such a cell for practical application, the flexible lithium metal battery was connected to a LED bulb (Fig. 5b). Obviously, the cell is functioning well both in flat as well as in highly bent states, hence, proofing the concept of our flexible battery that maintains its electrochemical characteristics under severe bending stress.

To validate the electrochemical performance of the flexible lithium metal battery, constant current cycling at 0.1 C was carried out (Fig. 6a). The initial discharge capacity of the flexible NVO

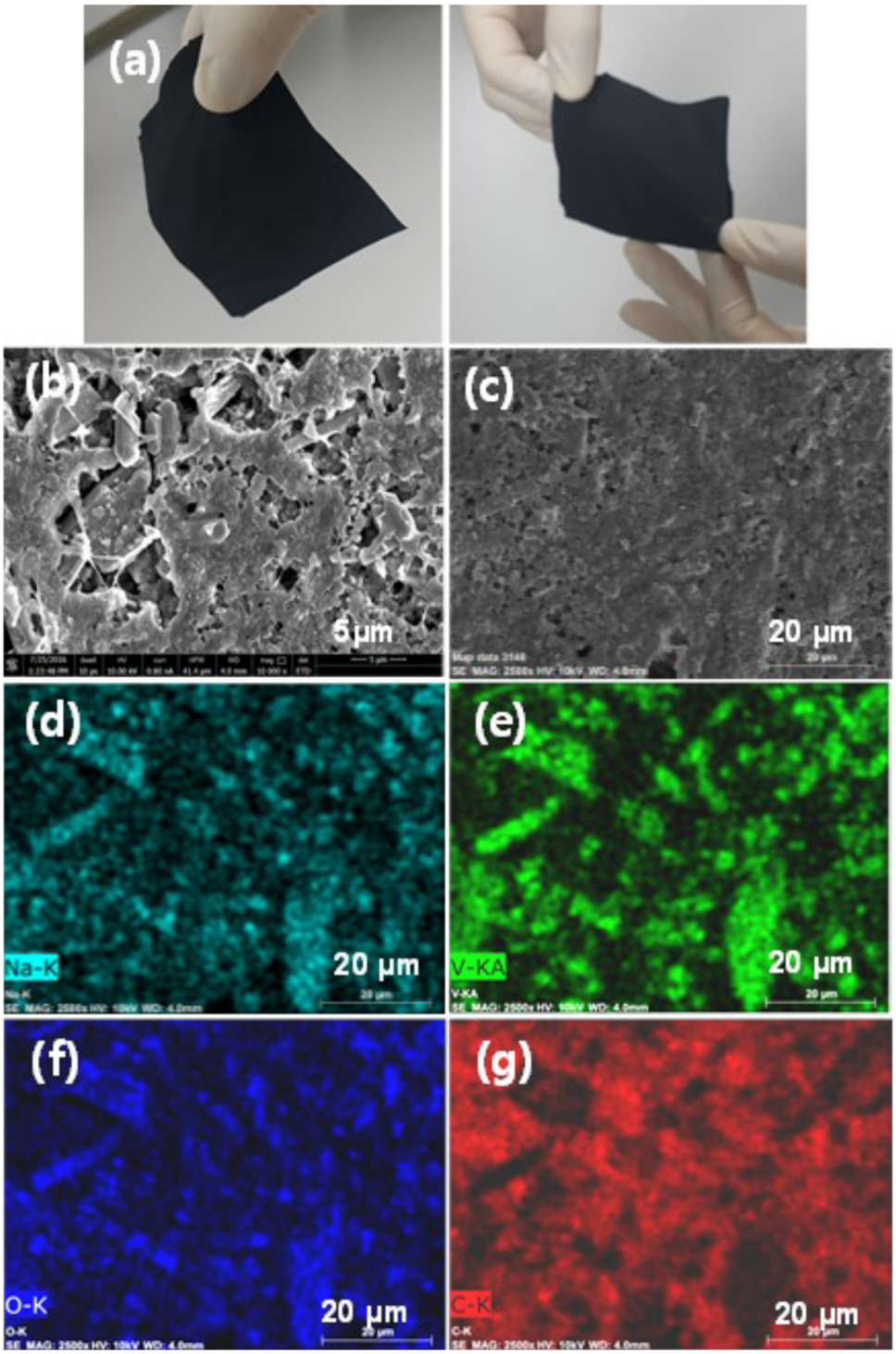

Fig. 4. (a) Photographs and (b) SEM micrograph of the free-standing electrode with (c-g) EDS elemental mapping. (c) Corresponding electron image, (d) sodium (Na), (e) vanadium (V), (f) oxygen (O) and (g) carbon (C) signals.

cathode was found to be as high as 228 mA h g^{-1}, which increases slightly to 233 mA h g^{-1} during the second cycle, after which it remains practically constant. The discharge value is corresponding to 99.6% of the theoretical capacity based on $Li_xNa_{0.33}V_2O_5$, with $0 \leq x \leq 1.66$. The Coulombic efficiency follows the same trend and increases from 97.9% (1st cycle) to almost 99.9% (2nd cycle) while it stabilizes with small fluctuations around 99.4% after 5 cycles (Fig. 6b). After 100 cycles, the discharge capacity decreased to 205.0 mA h g^{-1} (ca. 1.46 Li per mole) corresponding to an average fading of 0.23% per cycle. The specific energy densities are as high 407.8 Wh kg^{-1} at initial discharge and still remarkable 358.8 W h kg^{-1} at the 100th cycle (on electrode level). During extended cycling, the flexible lithium metal battery can maintain 89% of its initial (dis)charge capacity and high Coulombic efficiency close to 99.2% after the tested 100 low rate cycles, which implies an excellent reversibility of the flexible battery system. For increasing current densities, a decrease in specific capacity was observed going from 0.1C (228 mA h g^{-1}) to 5 C (106 mA h g^{-1}). The

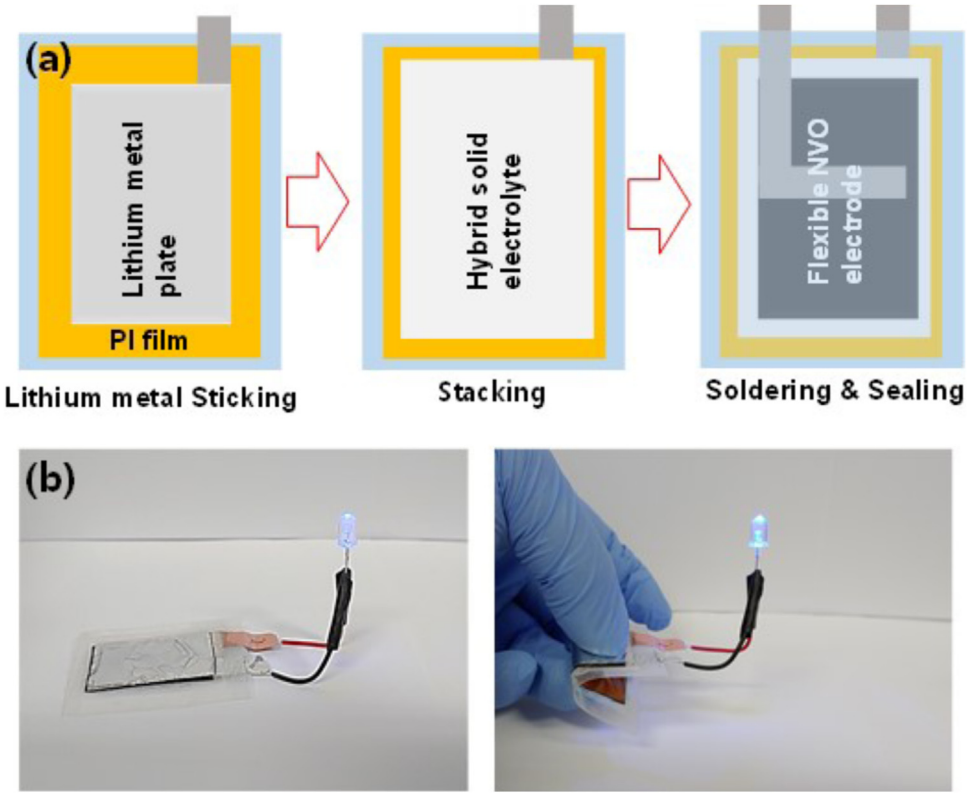

Fig. 5. (a) Preparation of the flexible NVO-lithium metal battery and (b) photographs of the flexible lithium metal battery in flat and highly bent states.

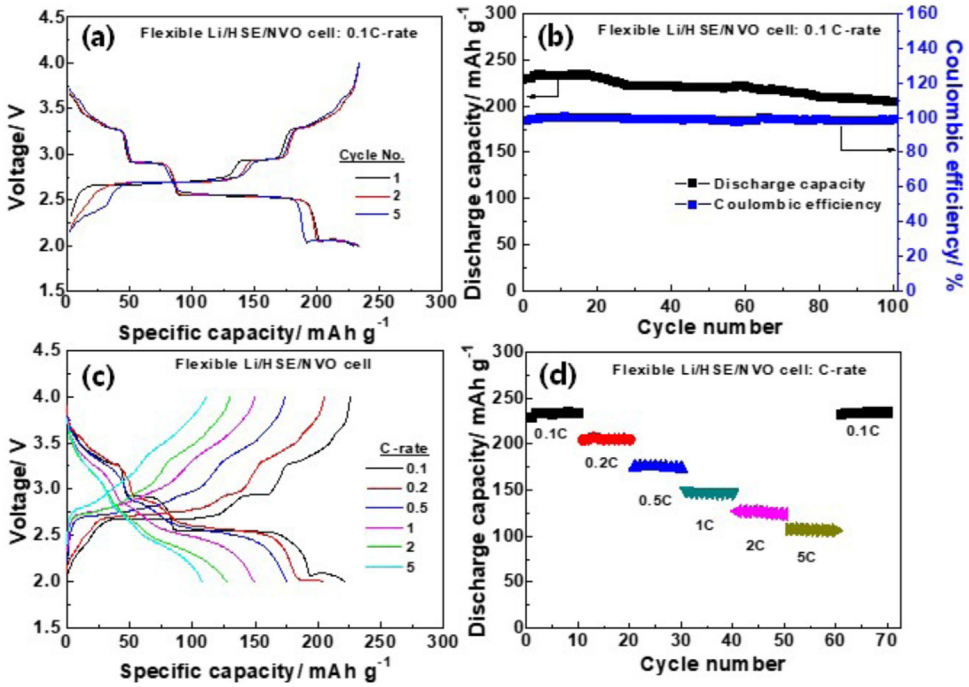

Fig. 6. Electrochemical performance of NVO-based flexible lithium metal battery. (a) Potential profiles for the first, second and 5th cycle for (b) constant current cycling at 0.1C. (c) Selected potential profiles during the (d) rate performance test under various current densities.

capacities obtained at high current density are almost the same as for typically reported NVO batteries, which in contrast to our work have a conductive coating applied and are using liquid electrolytes [31,32]. The high initial (dis)charge capacity can be retained when reverting back to lower rates (Fig. 6c, d) demonstrating the high reversibility and good flex-o-mechanical properties of the cell. This good rate capability of the integrated flexible metal battery provides the potential of fast charging and discharging for particular applications.

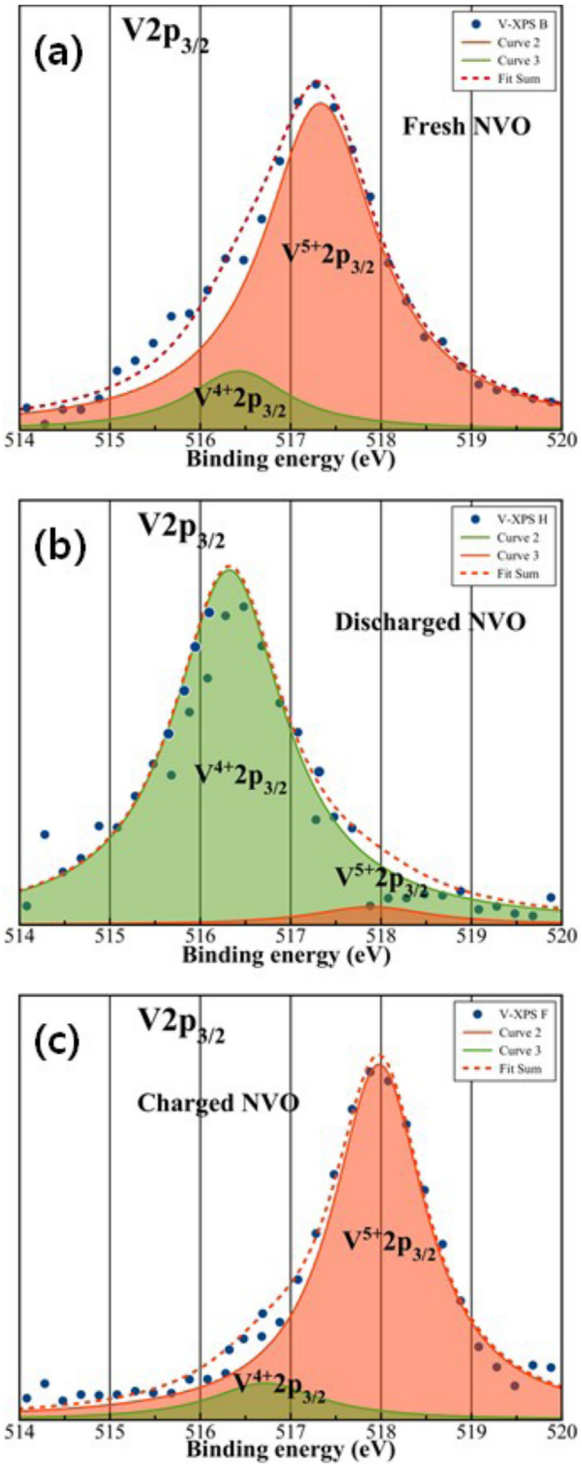

Fig. 7. Ex-situ XPS analysis of NVO electrodes at different states of (dis)charge during the first cycle. (a) Fresh NVO electrode, (b) discharged to 2.0 V, (c) charged to 4.0 V.

The redox processes in the NVO electrode during the first (dis) charge were investigated by ex-situ XPS of the vanadium region (Fig. 7). In the $V2p_{3/2}$ spectra, two peaks are present. They can be assigned to V^{4+} and V^{5+} and are located at 516.1 eV and 517.5 eV in the spectrum of the as-prepared NVO electrode, respectively [33]. After discharge, the V^{5+} peak decreased significantly and almost disappeared, while the intensity corresponding to V^{4+} has increased, implying reduction of NVO upon lithium-ion intercalation. After charge, the V^{4+}, as well as the V^{5+} peaks revert practically to their initial intensities confirming the high reversibility of the $V^{4+/5+}$ redox couple. During the electrochemical reaction, the peaks shift to slightly higher binding energies due to the intercalation of lithium ions into the structure [34].

Morphological characterization by SEM reveals the evolution of severe cracks in the active material particles upon cycling (Fig. 8). Micrographs taken of fresh electrodes (Fig. 8a) and electrode after 30, 50 and 100 cycles (Fig. 8b–d) nicely follow this behavior with cracks growing deeper into the particles until fracture. However, the principle particle morphology is maintained and ex-situ XRD (Fig. 8e) confirms the high structural stability of the material, which remains unchanged after 100 cycles. Therefore, the performance loss of the electrode is attributed to the particle fracturing of the NVO leading too poor ionic conductivity in the flexible cathode. This is supported by the electrochemical impedance spectra, recorded of the pristine electrode as well as after 50 and 100 cycles (Fig. 8f). The overall electrode resistance obtained from equivalent circuit fitting if the EIS spectra increases from around 130 Ω (fresh) to 230 Ω after 50 cycles and further to a value of 358 Ω after 100 cycles.

Thermal stability and safety of rechargeable batteries is an important asset, especially regarding wearable electronic devices but also electric vehicles. In a final step, the thermal stability of the flexible lithium metal battery using an NVO cathode and LAGP-based hybrid electrolyte, was evaluated at 60 °C (Fig. S5). The cell shows a stable (dis)charge capacity of 228 mA h g^{-1} over 20 cycles at 0.5 C, which is higher than the 175 mA h g^{-1} achieved at room temperature (compare Fig. 6c). Moreover, the initial Coulombic efficiency is as high as 99.1%. This dramatic performance improvement is ascribed to the better ionic conductivity of the hybrid electrolyte at this elevated temperature (see Fig. S3b) as well as reduced contact resistance between the electrodes and the electrolyte. Additionally, the higher thermal stability of the hybrid electrolyte (see Fig. S4) allows the flexible battery to run at such high temperatures with improved safety, unlike lithium-ion batteries employing liquid electrolytes [27]. Fig. S6 shows cycle performance of the flexible Li/HSE/NVO full-cell in bent (R = 3) and flat states. The specific capacity was maintained at 228.4 mA h g^{-1} after bending as compared with 233.6 mA h g^{-1} before bending (i.e., only a slight decrease of 2 %). In addition, the discharge capacity well recovered to 233.1 mA h g^{-1} when the flexible NVO cell was re-flattened. Such outstanding performance of the NVO-based flexible lithium metal battery will advance the possibilities of wearable electronic devices with high energy density and thermal stability.

Conclusions

We have designed and successfully fabricated a metal current collector-free flexible β-$Na_{0.33}V_2O_5$ (NVO) cathode and flexible lithium metal battery employing a $Li_{1.5}Al_{0.5}Ge_{1.5}P_3O_{12}$ (LAGP)-based hybrid electrolyte. Flexible NVO cathodes are prepared by a simple one step phase inversion technique with PVdF as binder. This approach appears very beneficial as it avoids the use of any post treatment or the introduction of an additional diffusion layer. Besides, the good chemical stability and physical robustness of PVdF further improves the flexibility of the NVO cathodes. Such integrated flexible batteries exhibit fast and stable lithium-ion storage capabilities, with high capacities (228 mA h g^{-1} at 0.1C and 106 mA h g^{-1} at 5 C) and good cycling stability (90% capacity retention after 100 low-rate cycles) translating into an outstanding specific energy of 407.8 W h kg^{-1}. This good electrochemical performance is attributed to a suitable degree of crystallinity of the dense nano-sized NVO with high structural stability. Moreover, the uniform distribution of NVO, conductive carbon and binder throughout the electrode ensures fast electron transfer within the

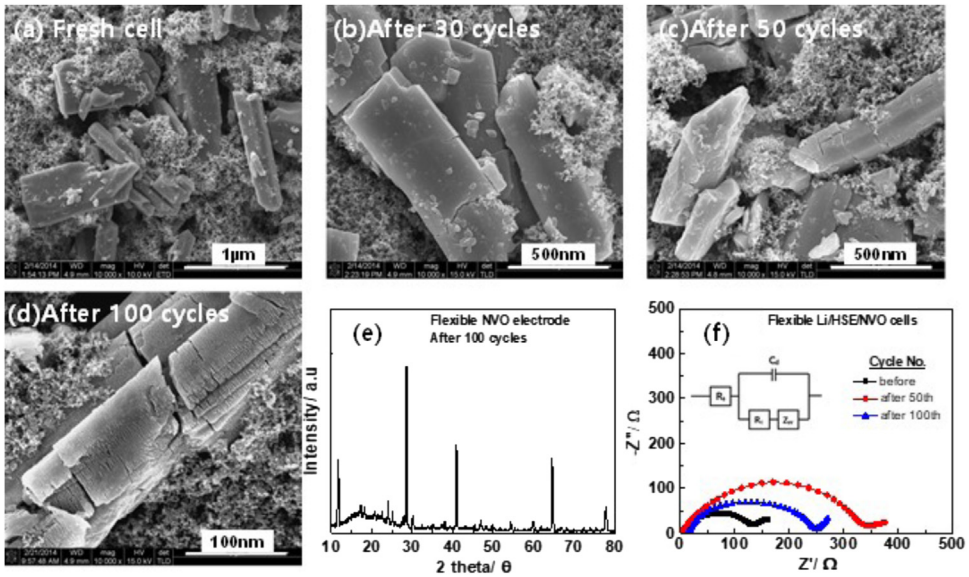

Fig. 8. SEM micrographs of (a) fresh NVO electrodes and (b–d) over cycling. (e) XRD pattern of an NVO electrode after 100 cycles and (f) EIS plots before cycling in comparison to after the 50th and 100th cycle. The equivalent circuit used for fitting is shown as an inset.

electrode and lithium-ion transfer through the LAGP-based hybrid electrolyte of high ionic conductivity. Finally, the NVO-based flexible lithium metal battery exhibits high thermal stability functioning well and safely at 60 °C with stable cycling and a high discharge capacity of 228 mA h g^{-1} at 0.5 C. The herein presented concept for high energy density and high thermal stability flexible batteries will open new possibilities for flexible energy storage devices in health-care and wearable electronics.

Declaration of interest statement

We have designed and successfully fabricated a metal current collector-free flexible β-$Na_{0.33}V_2O_5$ (NVO) cathode and flexible lithium metal battery employing a $Li_{1.5}Al_{0.5}Ge_{1.5}P_3O_{12}$ (LAGP)-based hybrid solid electrolyte. Typically, flexible lithium ion batteries have low energy density due to flexibility limitation of the electrodes. However, the flexible battery using a metal current collector-free NVO cathode combined with lithium metal anode can have high energy density. Lithium metal anode is not very flexible and does not return into its initial state once it was bent but we solved the problem by a simple method. The developed flexible batteries exhibit fast and stable lithium-ion storage capabilities, with high capacities (228 mA h g^{-1} at 0.1C and 106 mA h g^{-1} at 5 C) and good cycling stability (90% capacity retention after 100 low-rate cycles) translating into an outstanding specific energy of 407.8 W h kg^{-1}. Moreover, the flexible NVO-based lithium metal battery shows excellent electrochemical performance even at elevated temperature (60 °C) and bended-state employing a hybrid solid electrolyte.

Acknowledgements

This research was financially supported by the Basic Science Research Program through the National Research Foundation of Korea (NRF) funded by the Ministry of Education (2018R1A4A1024691 and 2020R1A2C2009057). Furthermore, M. K. would like to acknowledge financial support from the German Federal Ministry of Education and Research in the ExcellBattUlm project under contract number 03XP0257D. The financial support of the Helmholtz Association is also acknowledged.

Appendix A. Supplementary data

Supplementary material related to this article can be found, in the online version, at doi:https://doi.org/10.1016/j.jiec.2020.11.011.

References

[1] A. Manthiram, X. Yu, S. Wang, Nat. Rev. Mater. 2 (2017) 1.
[2] Q. Zhang, E. Uchaker, S.L. Candelaria, G. Cao, Chem. Soc. Rev. 42 (2013) 3127.
[3] M. Armand, J.-M. Tarascon, Nature 451 (2008) 652.
[4] M.S. Balogun, H. Yang, Y. Luo, W. Qiu, Y. Huang, Z.Q. Liu, Y. Tong, Energy Environ. Sci. 11 (2018) 1859.
[5] K. Amin, Q. Meng, A. Ahmad, M. Cheng, M. Zhang, L. Mao, K. Lu, Z. Wei, Adv. Mater. 30 (2018)1703868.
[6] Q. Meng, H. Wu, L. Mao, H. Yuan, A. Ahmad, Z. Wei, Adv. Mater. Technol. 2 (2017) 1.
[7] H. Cha, J. Kim, Y. Lee, J. Cho, M. Park, Small 14 (2018) 1.
[8] H. Luo, C. Xu, B. Wang, F. Jin, L. Wang, T. Liu, Y. Zhou, D. Wang, Electrochim. Acta 313 (2019) 10.
[9] S. Cao, L. Shi, M. Miao, J. Fang, H. Zhao, X. Feng, Electrochim. Acta 298 (2019) 22.
[10] J.-K. Kim, J. Manuel, M.-H. Lee, J. Scheers, D.-H. Lim, P. Johansson, J.-H. Ahn, A. Matic, P. Jacobsson, J. Mater. Chem. 22 (2012) 15045.
[11] S. Jessl, D. Beesley, S. Engelke, C.J. Valentine, J.C. Stallard, N. Fleck, S. Ahmad, M. T. Cole, M. De Volder, Mater. Sci. Eng. A 735 (2018) 269.
[12] M. Koo, K.I. Park, S.H. Lee, M. Suh, D.Y. Jeon, J.W. Choi, K. Kang, K.J. Lee, Nano Lett. 12 (2012) 4810.
[13] S. Ahmad, D. Copic, C. George, M. De Volder, Adv. Mater. 28 (2016) 6705.
[14] S. Song, S.W. Kim, D.J. Lee, Y.G. Lee, K.M. Kim, C.H. Kim, J.K. Park, Y.M. Lee, K.Y. Cho, ACS Appl. Mater. Interfaces 6 (2014) 11544.
[15] M.S. Whittingham, J. Electrochem. Soc. 123 (1976) 315.
[16] C. Delmas, S. Brèthes, M. Ménétrier, J. Power Sources 34 (1991) 113.
[17] C. Cartier, A. Tranchant, M. Verdaguer, R. Messina, H. Dexpert, Electrochim. Acta 35 (1990) 889.
[18] T. Zhai, H. Liu, H. Li, X. Fang, M. Liao, L. Li, H. Zhou, Y. Koide, Y. Bando, D. Golberg, Adv. Mater. 22 (2010) 2547.
[19] L. Mai, L. Xu, C. Han, X. Xu, Y. Luo, S. Zhao, Y. Zhao, Nano Lett. 10 (2010) 4750.
[20] M. Gödickemeier, L.J. Gauckler, J. Electrochem. Soc. 145 (1998) 414.
[21] Y. Xu, X. Han, L. Zheng, W. Yan, Y. Xie, J. Mater. Chem. 21 (2011) 14466.
[22] P.-P. Wang, C.-Y. Xu, F.-X. Ma, L. Yang, L. Zhen, RSC Adv. 6 (2016) 105833.
[23] S. Liang, J. Zhou, G. Fang, C. Zhang, J. Wu, Y. Tang, A. Pan, Electrochim. Acta 130 (2014) 119.
[24] W. Yang, W. He, F. Zhang, M.A. Hickner, B.E. Logan, Environ. Sci. Technol. Lett. 1 (2014) 416.
[25] R. Baddour-Hadjean, S. Bach, N. Emery, J.P. Pereira-Ramos, J. Mater. Chem. 21 (2011) 11296.
[26] J.K. Feng, L. Lu, M.O. Lai, J. Alloys Compd. 501 (2010) 255.
[27] J.K. Kim, Y.J. Lim, H. Kim, G.B. Cho, Y. Kim, Energy Environ. Sci. 8 (2015) 3589.
[28] H.T. Evans, J.M. Hughes, Am Mineral. 75 (1990) 508.
[29] J.K. Kim, B. Senthilkumar, S.H. Sahgong, J.H. Kim, M. Chi, Y. Kim, ACS Appl. Mater. Interfaces 7 (2015) 7025.
[30] Z. Lyu, G.J.H. Lim, R. Guo, Z. Pan, X. Zhang, H. Zhang, Z. He, S. Adams, W. Chen, J. Ding, J. Wang, Energy Storage Mater. 24 (2020) 336.

[31] F. Tian, L. Liu, Z. Yang, X. Wang, Q. Chen, X. Wang, Mater. Chem. Phys. 127 (2011) 151.
[32] N.H. Idris, M.M. Rahman, J.-Z. Wang, Z.-X. Chen, H.-K. Liu, Compos. Sci. Technol. 71 (2011) 343.
[33] I. Seo, G.C. Hwang, J.K. Kim, Y. Kim, Electrochim. Acta 193 (2016) 160.
[34] K. Liu, Q. Tan, L. Liu, J. Li, Environ. Sci. Technol. 53 (2019) 9781.